Title

A Catalytically Disabled Double Mutant of Src Tyrosine Kinase Can Be Stabilized into an Active-Like Conformation

Journal

Journal of Molecular Biology, 430(6)

ISSN

0022-2836

Authors

Meng, Yilin
Ahuja, Lalima G
Kornev, Alexandr P
et al.

Publication Date

2018-03-01

DOI

10.1016/j.jmb.2018.01.019

Peer reviewed

HHS Public Access

Author manuscript

J Mol Biol. Author manuscript; available in PMC 2019 March 16.

Published in final edited form as:

J Mol Biol. 2018 March 16; 430(6): 881–889. doi:10.1016/j.jmb.2018.01.019.

A Catalytically Disabled Double Mutant of Src Tyrosine Kinase Can Be Stabilized into an Active-Like Conformation

Yilin Meng[1], **Lalima G. Ahuja**[2], **Alexandr P. Kornev**[2], **Susan S. Taylor**[2,3], and **Benoît Roux**[1]

[1]**Department of Biochemistry and Molecular Biology,** University of Chicago, Chicago, IL 60637, USA

[2]**Department of Pharmacology,** University of California at San Diego, La Jolla, CA 92093, USA

[3]**Department of Chemistry and Biochemistry,** University of California at San Diego, La Jolla, CA 92093, USA

Abstract

Tyrosine kinases are enzymes playing a critical role in cellular signaling. Molecular dynamics umbrella sampling potential of mean force computations are used to quantify the impact of activating and inactivating mutations of c-Src kinase. The potential of mean force computations predict that a specific double mutant can stabilize c-Src kinase into an active-like conformation while disabling the binding of ATP in the catalytic active site. The active-like conformational equilibrium of this catalytically dead kinase is affected by a hydrophobic unit that connects to the hydrophobic spine network via the C-helix. The αC-helix plays a crucial role in integrating the hydrophobic residues, making it a hub for allosteric regulation of kinase activity and the active conformation. The computational free-energy landscapes reported here illustrate novel design principles focusing on the important role of the hydrophobic spines. The relative stability of the spines could be exploited in future efforts to artificially engineer active-like but catalytically dead forms of protein kinases.

Keywords

free-energy landscape; molecular dynamics; conformational change; catalysis

Introduction

Protein kinases are crucial molecular components of cellular signaling pathways regulating cell growth, proliferation, metabolism, differentiation, and migration. In their active state, protein kinases catalyze the transfer of γ-phosphate of an adenosine triphosphate (ATP) molecule covalently onto substrate proteins and peptides. However, recent studies suggest that protein kinases are not primarily optimized to function as efficient catalytic enzymes, but as dynamical allosteric structures serving as molecular switches to regulate cellular

Correspondence to Benoît Roux: roux@uchicago.edu.

Appendix A. Supplementary Data

Supplementary data to this article can be found online at https://doi.org/10.1016/j.jmb.2018.01.019.

signaling [1,2]. The mechanisms by which different kinases toggle between inactive and active states are very diverse and kinase-dependent. Two conserved structural element, the regulatory (R) and catalytic (C) “hydrophobic spines” shown in Fig. 1a, represent an important unifying functional feature of the eukaryotic protein kinase superfamily [2]. An active kinase is associated with an assembled R-spine, and the completion of the C-spine by binding of ATP into the active site cleft allows for priming the kinase for catalysis.

In recent years, the allosteric regulation of protein kinase activities has attracted much attention. Insights into the allosteric activation of kinases have been revealed through the investigation of a broad range of protein kinases such as tyrosine kinase c-Abl [3–5], c-Src [5–8], and the EGFR family [9]. In a model explaining the *trans*-activation (dimerization-dependent mechanism), one kinase serves as the receiver that is being activated, while the other serves as the activator [9]. Remarkably, a working enzymatic active site is not required for the activator—the latter can be a catalytically dead kinase, for example, B-Raf inhibited by vemurafenib [10] or pseudokinase ERBB3 [11]. Non-receptor tyrosine kinase c-Src has been utilized as a prototypical system to study the allosteric regulation. The dynamic coupling between the ATP-binding site, substrate-binding site, and the regulatory motifs in the kinase domain has been probed by both experimental and computational techniques. Foda *et al.* [6] combined NMR technique with molecular dynamics (MD) simulations to investigate cellular signal relay in Src. They have identified an allosteric network for the signal relay. Furthermore, they have also discovered that ATP and substrate peptide bind in a negative cooperative fashion. A recent study from the Seeliger lab further monitors the effect of conformationally selective inhibitors on kinase backbone dynamics by NMR spectroscopy, and discovered that the induced dynamic changes occur across the entire kinase [8]. This study also probed how the regulatory SH3–SH2 domains perturb the kinase domain experimentally, while a recent study by Fajer *et al.* [12] investigated the effect computationally. In a parallel study, Pucheta-Martínez *et al.* [7] utilized a combination of solution NMR and enhanced sampling MD simulations to investigate the cross-talk between the ATP-binding site and the activation loop (A-loop) in Src kinase. They have discovered that A-loop phosphorylation and ATP binding are necessary to achieve the fully active state, and the phosphorylation has a significant allosteric effect on the C-lobe. Furthermore, their computational and NMR work have demonstrated that the phosphorylation of A-loop rigidifies Src kinase, which is consistent with the findings from an earlier computational study using umbrella sampling simulations [7,13]. The investigation of allosteric activation also has pharmacological importance: for example, the resistance to B-Raf inhibitor vemurafenib is attributed to the allosteric activation of B-Raf and the formation of stable B-Raf homodimer and B-Raf*C-Raf heterodimer [10,14]. The next-generation B-Raf inhibitors were designed to inhibit the allosteric activation [15]. Recently, Lovera *et al.* [5] combined MD simulations with *in vitro* mutagenesis and microcalorimetry to investigate the resistance to protein kinase inhibitor imatinib in Abl mutants, and revealed an allosteric effect of the drug-resistant single point mutations.

The role of a non-catalytic kinase in the dimerization-dependent activation mechanism demonstrates that the scaffolding action of a kinase domain is itself capable of critical functional role in cellular signal transduction—even when the catalytic machinery is disabled. Experimentally, it can be difficult to separate the catalytic and scaffolding

functional signal from a kinase, especially when the latter is associated with the active conformation [16]. Such kinase constructs achieve a separation of the active protein conformation from any catalytic activity, and thus can serve as powerful investigative tools.

To discover if these ideas are generalizable, an important question is whether one could computationally engineer models of catalytically dead kinases locked in an active conformation. To address this question, the c-Src kinase domain can serve as a useful prototypical system. Previous computational studies based on two-dimensional (2D) umbrella sampling calculations were used to characterize the conformational equilibrium in the c-Src kinase domain, yielding results in excellent agreement with experiments [12, 13, 17, 18]. Encouraged by this success, we decided to apply the same approach to explore the effect of mutations on the free-energy landscape of the catalytic domain of c-Src.

Results and Discussion

All mutants of c-Src were characterized on the basis of 2D potential of mean force (2D-PMF) umbrella sampling calculations. The resulting free-energy landscapes are shown in Fig. 2. We first discuss two single mutants, M314V and L297F (chicken c-Src numbering is used throughout this work), chosen on the basis of results obtained with B-Raf in previous studies [19–21]. The M314 residue is the RS3 position in the R-spine and serves as the fulcrum between the R-spine and the αC helix. In Raf kinases, this residue is a smaller aliphatic moiety (L505 in B-Raf and L397 in C-Raf), and its mutation to a bulkier residue like phenylalanine or a more hydrophobic residue like methionine allows for constitutive catalytic activity [21]. The manipulation of this RS3 residue allows for activation of RAFs and other tyrosine-like kinases independent of their activator-receiver mechanism. Similarly, the L297F position in RAFs is seen to have a similar effect that probably allows for the engaging of the αC helix and the R-spine. Mutations in this residue are found to be activating and are associated with the cardio-facio-cutaneous syndrome [20]. Like in the case of B-Raf, mutation of the corresponding methionine to a residue with a smaller side chain in c-Src is observed to reduce or ablate the catalytic activity presumably because disassembling the R-spine is easier [19]. The two mutations, which are known to have opposite inactivating and activating impact on the conformational equilibrium of the kinase, can serve to test the reliability of the computations as a negative and positive control, respectively. The calculated free-energy landscapes of the single mutants, displayed in panels a–c in Fig. 2, are consistent with experimental observations on B-Raf. The active-like conformation in the M314V construct indeed has a much higher free energy than the inactive conformation when compared with the wild-type (WT) construct (Fig. 3A of Ref. [13]), which would lead to a reduced catalytic activity. The computations underlie the importance of the R-spine with respect to the relative stability of the active/inactive conformation: the M314V reduces catalytic activity because it makes it easier to disassemble the R-spine. Furthermore, the introduction of a phenyl group at the L297 position allows it to make stacking interactions with the F307 of the αC helix, allowing this interacting to prevent the outward movement of the helix as seen in the inactive Src conformation. This mutation ensures the constitutive assembly of the R-spine, such that equilibrium between the inactive state (R-spine disassembled) and active state (R-spine assembled) is in favor of locking the kinase in an active state. By analogy, it is worth noting that a conserved

tryptophan in B-Raf (W450) also extends the R-spine by forming stacking interactions stabilizing the active state [22,23], although the residue corresponding to W450 in Src is W260, which was not mutated in the present study. Consistent with this analysis, the free-energy landscapes of the two L297F constructs (Fig. 2b, c) demonstrate that L297F provides the essential interactions to lock the kinase in its active-like conformation. The purpose of performing umbrella sampling calculations for the L297F with ATP-Mg^{2+} construct is to evaluate the impact of adding ATP and Mg^{2+} on the free-energy landscape. Phosphorylation of the A-loop is not needed. Hence, the L297F single mutant should display high catalytic activity. The 2D umbrella sampling calculations on c-Src are able to reflect the trends experimentally observed on B-Raf.

Having verified that the computational strategy is sound, we sought to engineer a form of Src kinase that is active-like but catalytically dead. Inspired by the A481F mutation in B-Raf kinase, which is known to disrupt ATP binding and break the C-spine but retains the ability to dimerize and activate the RAF–MEK–ERK signaling pathway [16], we examined possible mutation of the residue at the corresponding position in c-Src, Val281. We first considered the V281F single mutant, in the hope that it could yield the same outcome in c-Src as A481F in B-Raf. However, the free-energy landscape of V281F (Fig. 2d) resembles that of the unphosphorylated WT Src (Fig. 3A in Ref. [13]). The active-like conformation appears to be slightly stabilized by the mutation, suggesting that V281F does not sufficiently shift the conformational equilibrium toward the active-like/inactive state. Nevertheless, the mutation would abolish catalytic activity by fusing the C-spine across the two kinase lobes and abrogating ATP binding in the active site.

To achieve a more complete stabilization of the active-like conformation of the kinase, a second point mutation is required. The L297F mutation, on the basis of its free-energy landscape (Fig 2b), appears as a promising candidate. Accordingly, the double mutant of Src, V281F–L297F, should be catalytically disabled due to the fused C-spine, and also locked in the active-like conformation. This prediction is confirmed by the computations. The free-energy landscape of the V281F–L297F construct (Y416 in the A-loop is unphosphorylated) is shown in Fig. 2e. The free-energy landscapes of the double mutant resemble that of the L297F, showing only one deep free-energy basin, which corresponds to the active-like state. Only the active-like conformation of V281F–L297F is stable, even after the free-energy threshold used in the self-learning adaptive umbrella sampling computation [24] is increased to 20 kcal/mol. This energy cutoff is sufficiently high to overcome barriers and to discover intermediate and inactive states according to the free-energy landscape obtained from previous umbrella sampling simulations of the WT Src kinase domain with Y416 unphosphorylated [13,17]. Therefore, the free-energy PMF calculation indicates that the V281F–L297F double mutant is essentially “locked” into an active-like state, although the A-loop is not phosphorylated. From a conformational stability point of view as reported by the PMF, the mutations achieve a similar effect to that of phosphorylating Y416 in the A-loop (see Fig. 3B in Ref. [13]). A question naturally arisen is that what could happen when both M314V and L297F are introduced. Free-energy landscape (Fig. 2f) of the L297F–M314V double mutant shows a compromise between the two opposing effects. Hence, the stability of the inactive/active-like conformation can be maximized when both the hydrophobic unit and the R-spine are synergized.

Structurally, the V281F–L297F mutant behaves essentially “as if” the A-loop is phosphoryated [13]. The sharp rise in free energy suggests that the double-mutant kinase is unlikely to rotate the αC helix outward or to disassemble the R-spine, and as a result, the active-like conformation is very stable. The one-dimensional (1D)-PMF calculated as a function of the RMSD of the R-spine relative to the 1Y57 conformation is shown in Fig. 3. It suggests that the R-spine is stabilized in the active conformation (the assembled “on” conformation) for V281F–L297F, indicated by only one energy basin observed in the PMF. A similar behavior is also observed in the WT Src kinase with its A-loop phosphorylated [13]. This effect could have crucial impacts on performing the scaffolding function, for example, an inward rotation is needed to form the dimer of active EGFR [9].

To verify that the V281F mutation should yield a non-catalytic Src kinase, an unbiased 46 ns MD simulation of the V281F–L297F construct was carried out. The snapshots of the trajectory were aligned with respect to a reference structure corresponding to the WT kinase domain in an active-like conformation with bound ATP and Mg^{2+}. The reference structure is based on the PDB ID 1Y57 [25]. Figure 1b shows the reference structure superimposed with a representative snapshot from the double mutant V281F–L297F. In the mutant kinase, the Phe at position 281 clashes with the adenine group and the ribose of the ATP from the reference structure. The distance between the Hζ atom of F281 and the N7, C8, N9 atoms of ATP as well as the distance between the Hε atoms of F281 and the C1′ and O4′ atoms of ATP are calculated and plotted in Supp. Fig. S1. The distance between Hε and O4′ and C1′ is 2.0 ± 0.7 and 2.5 ± 0.8 Å, respectively. The distance between Hζ and N7, C8, N9 is 2.7 ± 1.2, 2.5 ± 0.9, and 3.0 ± 0.8 Å, respectively. Longer unbiased simulations confirmed these observations. It follows that F281 is constantly occupying the ATP-binding site. Therefore, it would disrupt, or even abolish, ATP binding if the ATP molecule were present. However, the actual impact of V281F point mutation on ATP binding needs to be probed with binding free-energy calculations, and is not the subject of this article.

To provide further molecular details of F297 in the V281F–L297F double mutant, the non-bonded interaction energies between F297 and the rest of the protein are calculated. E(F297, i) as a function of residue index (i) are displayed in Supp. Fig. S2A. F297 couples very strongly with F278, P299, P304, F307, and I334 when the αC-helix is rotated inward. The MD equilibration trajectory explores the free-energy basin (Supp. Fig. S2B). Figure 4a shows a cartoon representation of this cluster of residues. Those residues also belong to a hydrophobic community referred to as the αC-helix positioning community (Supp. Fig. S3) [26,27], which links the P-loop to the αC-helix. The L297F mutation is found to strengthen intra-community interactions and stabilize the inward-rotated αC-helix (see Fig. S4). Interestingly, F297, as well as the hydrophobic cluster, is strongly coupled with the R-spine. The αC-helix serves as a motif to integrate the hydrophobic cluster with the R-spine (shown in Fig. 4b) so that the L297F mutation is also able to stabilize the assembly of the R-spine. This renders the αC-helix a hub for allosteric regulation of the kinase activity.

Further analysis of the C-spine residues was carried out on the basis of the 46-ns trajectory. As illustrated in Fig. 5a, both the N-lobe (F281 and A293) and the C-lobe (I392–L393–V394–L346–L451–L455) portions of the C-spine are always connected within each lobe. However, when F281 is connected with L393, the entire C-spine is completed (left panel,

Fig. 5a), while a gap can be seen (right panel, Fig. 5a) if F281 and L393 are further away. Therefore, the van der Waals (vdW) energy between F281 and L393 is calculated for each frame in the 46-ns trajectory. Distribution of the vdW interaction energy between C-spine residues in the N-lobe and those in the C-lobe (F281 and L393) also confirms that the C-spine is fused when F281 is present (see Fig. 5b). Therefore, mutating V281 to F281 indeed disrupts ATP binding and fuses the C-spine, leading to a catalytically inactive Src kinase.

Conclusion

The present results suggest that the concept of conformationally active but catalytically dead kinases may be generalized. MD PMF simulations predict that a double mutant of Src, V281F–L297F, should be catalytically disabled due to a fused C-spine and simultaneously locked in an active-like conformation through the hydrophobic engagement of the R-spine via the αC helix. These computations illustrate novel design principles that could be exploited to engineer catalytically dead kinases locked in an active-like conformation through a stabilization of the hydrophobic spines. The possibility to engineering mutations achieve a separation of the active protein conformation from any catalytic activity makes this double c-Src mutant a promising model that could be used to further investigate the functional role of scaffolding in signaling kinase and other non-catalytic roles.

Materials and Methods

Atomic models and MD simulation

The construction of the initial structure used PDB 1Y57 as a template. For the sake of simplicity, only residues from Gln253 to Thr523 were included in the construct, as illustrated in Fig. S3. The inhibitor and the sulfate ion were removed from the system. Residue V281 and L297 were mutated to phenylalanine. Since the point mutation at residue 281 from Val to Phe is believed to make the kinase unable to bind ATP, no ATP or Mg^{2+} was added to the construct. The all-atom system was solvated in a cubic simulation cell constructed from an equilibrated 86 × 86 × 86 $Å^3$ box of TIP3P water molecules; the system comprises 15,013 water molecules in total. The size of the simulation cell was chosen to extend at least 10 Å away from the surface of the protein. In addition, 45 K^+ ions and 42 Cl^- ions were inserted into the system to neutralize the total charge and to model a salt concentration of approximately 150 mM. This system is referred to as the V281F–L297F for future references. The initial V281F–L297F with unphosphorylated A-loop was relaxed and equilibrated in the following protocol: energy minimization was carried out for 2000 steps using the steepest-descent algorithm; next, the system was equilibrated for 500 ps with all heavy atoms of the protein restrained to their initial positions; V281F–L297F was further relaxed for 2 ns with all backbone atoms of the protein restrained to their initial positions; then the system was equilibrated for another 46 ns completely unrestrained. The unbiased 46 ns of equilibration period formed the basis of pre-umbrella sampling analysis.

All energy minimization and MD propagations (including umbrella sampling calculations) were performed using version 2.9 of the molecular simulation package NAMD with the all-atom CHARMM36 force field. The isobaric–isothermal (NPT) ensemble was employed for all MD calculations. The pressure and temperature were controlled by Langevin piston

method and Langevin dynamics and kept at 1 atm pressure and 300 K, respectively. Periodic boundary conditions were applied and Particle Mesh Ewald was used to treat long-range non-bonded interactions. The short-range non-bonded interactions were truncated at 12 Å, with a switching function turned on from 10 to 12 Å. Covalent bonds involving hydrogen atoms were constrained at their equilibrium distances so that a 2-fs time step was used throughout all simulations.

2D umbrella sampling simulation

Cartoon representations of the conformational change, which is the subject of the 2D umbrella sampling calculations and of the order parameters utilized to characterize the conformational change, are illustrated in Ref. [13]. The unphosphorylated active-like kinase domain used in all US calculations was based on the crystallographic structure 1Y57 of Src.

US calculations have been proved to be effective in understanding the conformational changes in Src-family kinases. The self-learning adaptive umbrella sampling calculations was used for the present computations [24]. The windows were launched for the V281F–L297F double mutant, starting from the active-like conformation (with unphosphorylated Y416 in the A-loop) with 60 windows. Initial structures were taken from the 46-ns equilibration simulation such that the selected snapshot is the closet to the window center. Technically, we employed a two-stage process. The first stage is growing the umbrella windows with the self-learn adaptive method. In this stage, 10 ns of MD sampling was utilized for each window. A free-energy threshold of 20 kcal/mol was used to ensure overcoming barriers, and 843 umbrella windows were finally used. Once the number of umbrella windows was determined, another 10 ns of sampling per window was carried out for all 843 windows in the second stage. All technical parameters of the 2D umbrella sampling calculations are given in Table 1. Therefore, we manually selected a subset of the 843 umbrella windows and performed the US calculations. The same rationale also applies to our umbrella sampling calculations of the L297F–M314V construct.

To save human and computer times, no self-learning adaptive process was applied to the rest of 2D umbrella sampling calculations and only a subset of the existing umbrella windows was used, with the exception of L297F and no ATP-Mg^{2+} construct in which all 843 windows from the V281F–L297F simulation were kept. One should also note that the M314V simulation was based on our WT 2D umbrella sampling. Therefore, ATP and Mg^{2+} were included in the simulation and the entire “L”-shaped landscape is shown. The weighted histogram analysis method was employed to combine time series from US calculations and to generate PMFs for all constructs. A total of 61.61 μs is accumulated for all 2D umbrella sampling. Details about the US simulations are given in Table 1. A total of 61.61 μs of aggregate MD data was accumulated for all 2D umbrella sampling for 2D-PMFs shown in Fig. 2.

Supplementary Material

Refer to Web version on PubMed Central for supplementary material.

Acknowledgments

This work was supported by the National Cancer Institute of the National Institutes of Health through Grant CAO93577. The computations are supported in part by the National Institutes of Health through resources provided by the Computation Institute and the Biological Sciences Division of the University of Chicago and Argonne National Laboratory under Grant 1S10OD018495-01, by the Extreme Science and Engineering Discovery Environment under Grant No. OCI-1053575, and by the University of Chicago Research Computing Center. The authors thank Dr. Christopher L. McClendon for his work on the community-map model of the Src kinase. The authors declare no conflict of interest.

Abbreviations used:

ATP	adenosine triphosphate
MD	molecular dynamics
WT	wild-type
vdW	van der Waals
HSQC	heteronuclear single quantum coherence
US	umbrella sampling
PMF	potential of mean force
NMR	nuclear magnetic resonance
A-loop	activation loop

References

[1]. Taylor SS, Ilouz R, Zhang P, Kornev AP, Assembly of allosteric macromolecular switches: lessons from PKA, Nat. Rev. Mol. Cell Biol. 13 (2012) 646–658. [PubMed: 22992589]

[2]. Shaw AS, Kornev AP, Hu JC, Ahuja LG, Taylor SS, Kinases and pseudokinases: lessons from RAF, Mol. Cell. Biol. 34 (2014) 1538–1546. [PubMed: 24567368]

[3]. Filippakopoulos P, Kofler M, Hantschel O, Gish GD, Grebien F, Salah E, et al., Structural coupling of SH2-kinase domains links fes and Abl substrate recognition and kinase activation, Cell 134 (2008) 793–803. [PubMed: 18775312]

[4]. Dolker N, Gorna MW, Sutto L, Torralba AS, Superti-Furga G, Gervasio FL, The SH2 domain regulates c-Abl kinase activation by a cyclin-like mechanism and remodulation of the hinge motion, PLoS Comput. Biol. 10 (2014), e1003863. [PubMed: 25299346]

[5]. Lovera S, Morando M, Pucheta-Martinez E, Martinez-Torrecuadrada JL, Saladino G, Gervasio FL, Towards a molecular understanding of the link between imatinib resistance and kinase conformational dynamics, PLoS Comput. Biol. 11 (2015), e1004578. [PubMed: 26606374]

[6]. Foda ZH, Shan YB, Kim ET, Shaw DE, Seeliger MA, A dynamically coupled allosteric network underlies binding cooperativity in Src kinase, Nat. Commun. 6 (2015) 5939. [PubMed: 25600932]

[7]. Pucheta-Martínez E, Saladino G, Morando MA, Martinez-Torrecuadrada J, Lelli M, Sutto L, et al., An allosteric cross-talk between the activation loop and the ATP binding site regulates the activation of Src kinase, Sci. Rep. 6 (2016), 24235. [PubMed: 27063862]

[8]. Tong M, Pelton JG, Gill ML, Zhang W, Picart F, Seeliger MA, Survey of solution dynamics in Src kinase reveals allosteric cross talk between the ligand binding and regulatory sites, Nat. Commun. 8 (2017) 2160. [PubMed: 29255153]

[9]. Jura N, Zhang XW, Endres NF, Seeliger MA, Schindler T, Kuriyan J, Catalytic control in the EGF receptor and its connection to general kinase regulatory mechanisms, Mol. Cell 42 (2011) 9–22. [PubMed: 21474065]

[10]. Poulikakos PI, Zhang C, Bollag G, Shokat KM, Rosen NRAF, inhibitors transactivate RAF dimers and ERK signalling in cells with wild-type BRAF, Nature 464 (2010) 427–430. [PubMed: 20179705]

[11]. Zhang XW, Gureasko J, Shen K, Cole PA, Kuriyan J, An allosteric mechanism for activation of the kinase domain of epidermal growth factor receptor, Cell 125 (2006) 1137–1149. [PubMed: 16777603]

[12]. Fajer M, Meng Y, Roux B, The activation of c-Src tyrosine kinase: conformational transition pathway and free energy landscape, J. Phys. Chem. B 121 (2016) 3352–3363. [PubMed: 27715044]

[13]. Meng Y, Roux B, Locking the active conformation of c-Src kinase through the phosphorylation of the activation loop, J. Mol. Biol. 426 (2014) 423–435. [PubMed: 24103328]

[14]. Rajakulendran T, Sahmi M, Lefrancois M, Sicheri F, Therrien M, A dimerization-dependent mechanism drives RAF catalytic activation, Nature 461 (2009) 542–545. [PubMed: 19727074]

[15]. Karoulia Z, Gavathiotis E, Poulikakos PI, New perspectives for targeting RAF kinase in human cancer, Nat. Rev. Cancer 17 (2017) 676. [PubMed: 28984291]

[16]. Hu JC, Yu HY, Kornev AP, Zhao JP, Filbert EL, Taylor SS, et al., Mutation that blocks ATP binding creates a pseudokinase stabilizing the scaffolding function of kinase suppressor of Ras, CRAF and BRAF, Proc. Natl. Acad. Sci. U. S. A. 108 (2011) 6067–6072. [PubMed: 21441104]

[17]. Meng Y, Lin YL, Roux B, Computational study of the “DFG-flip” conformational transition in c-Abl and c-Src tyrosine kinases, J. Phys. Chem. B 119 (2015) 1443–1456. [PubMed: 25548962]

[18]. Meng Y, Pond MP, Roux B, Tyrosine kinase activation and conformational flexibility: lessons from Src-family tyrosine kinases, Acc. Chem. Res. 50 (2017) 1193–1201. [PubMed: 28426203]

[19]. Azam M, Seeliger MA, Gray NS, Kuriyan J, Daley GQ, Activation of tyrosine kinases by mutation of the gatekeeper threonine, Nat. Struct. Mol. Biol. 15 (2008) 1109–1118. [PubMed: 18794843]

[20]. Rodriguez-Viciana P, Tetsu O, Tidyman WE, Estep AL, Conger BA, Cruz MS, et al., Germline mutations in genes within the MAPK pathway cause cardio-facio-cutaneous syndrome, Science 311 (2006) 1287–1290. [PubMed: 16439621]

[21]. Hu J, Ahuja LG, Meharena HS, Kannan N, Kornev AP, Taylor SS, et al., Kinase regulation by hydrophobic spine assembly in cancer, Mol. Cell. Biol. 35 (2015) 264–276. [PubMed: 25348715]

[22]. Jambrina PG, Bohuszewicz O, Buchete NV, Kolch W, Rosta E, Molecular mechanisms of asymmetric RAF dimer activation, Biochem. Soc. Trans. 42 (2014) 784–790. [PubMed: 25109958]

[23]. Jambrina PG, Rauch N, Pilkington R, Rybakova K, Nguyen LK, Kholodenko BN, et al., Phosphorylation of RAF kinase dimers drives conformational changes that facilitate transactivation, Angew. Chem. Int. Ed. Engl. 55 (2016) 983–986. [PubMed: 26644280]

[24]. Wojtas-Niziurski W, Meng Y, Roux B, Berneche S, Self-learning adaptive umbrella sampling method for the determination of free energy landscapes in multiple dimensions, J. Chem. Theory Comput. 9 (2013) 1885–1895. [PubMed: 23814508]

[25]. Cowan-Jacob SW, Fendrich G, Manley PW, Jahnke W, Fabbro D, Liebetanz J, et al., The crystal structure of a c-Src complex in an active conformation suggests possible steps in c-Src activation, Structure 13 (2005) 861–871. [PubMed: 15939018]

[26]. McClendon CL, Kornev AP, Gilson MK, Taylor SS, Dynamic architecture of a protein kinase, Proc. Natl. Acad. Sci. U. S. A. 111 (2014) E4623–E4631. [PubMed: 25319261]

[27]. Ahuja LG, Kornev AP, McClendon CL, Veglia G, Taylor SS, Mutation of a kinase allosteric node uncouples dynamics linked to phosphotransfer, Proc. Natl. Acad. Sci. U. S. A. 114 (2017) E931–E940. [PubMed: 28115705]

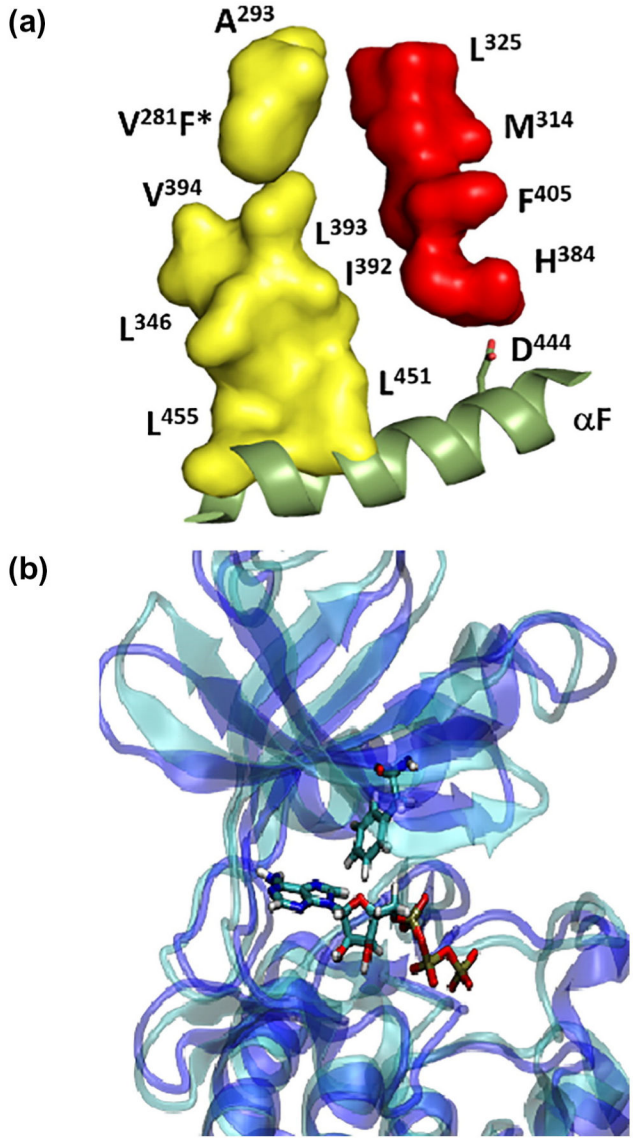

Fig. 1.

Structural details of c-Src kinase. (a) The hydrophobic spines in the Src kinase. The catalytic (C-) spine is colored in yellow and the regulatory (R-) spine is colored in red. The αF-helix is shown in olive color and serves as an anchor point. (b) A representative structure of V281F–L297F (colored in blue) overlapped with WT activelike Src kinase domain (the reference structure) which is based on 1Y57 (colored in cyan). The clash between F281 and the ATP molecule in the reference structure is shown.

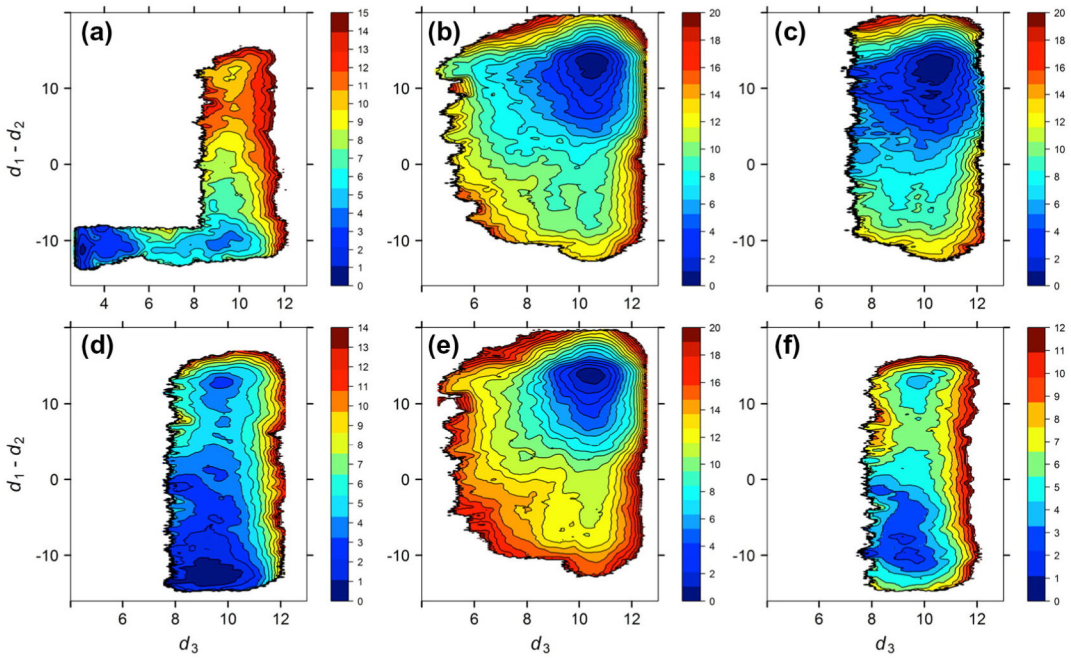

Fig. 2.

Free-energy landscapes of the Src kinase domain activation for various mutant constructs (energy levels are indicated in kcal/mol). Included are M314V (a), L297F without ATP + Mg^{2+} (b), L297F with ATP + Mg^{2+} (c), V281F (d), V281F–L297F (e), and L297F–M314V (f). The *y*-axis is chosen to reflect the motion of the αC helix and the assembly/disassembly of the R-spine as well, while the *x*-axis reflects the motion of the A-loop (see Ref. [13] for details about the order parameters). The free-energy basin at the top-right corner of the contour maps corresponds to the active-like conformation in which the αC helix is rotated inward and the A-loop is extended. In panel A, the free-energy basin at the lower-left corner of the contour map corresponds to the inactive conformation, while the one at lower-right corner is an intermediate state in which the αC helix is pointed outward but the A-loop is extended.

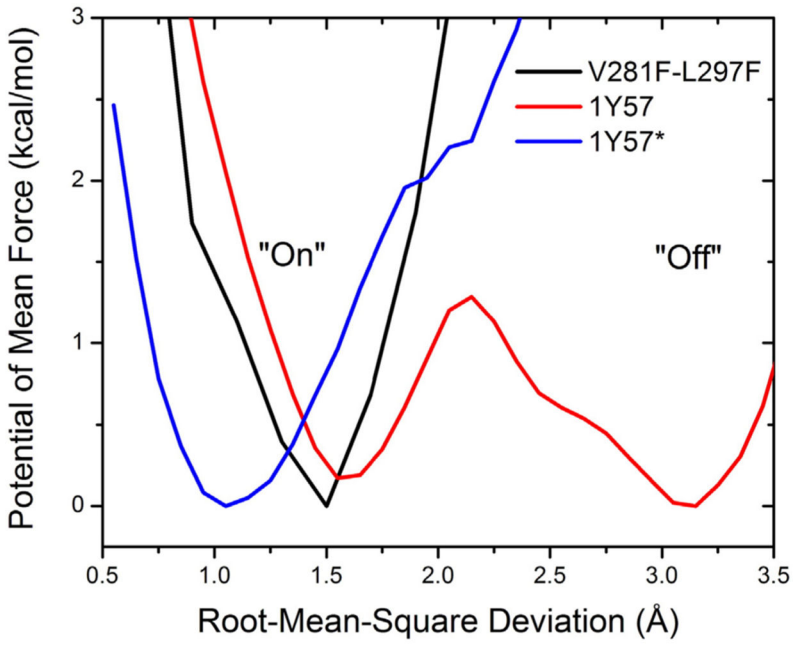

Fig. 3.

Free-energy profile as a function of the RMSD of the R-spine relative to the active-like conformation (PDB ID: 1Y57). All heavy atoms in the R-spine are used in the calculation of RMSD. The 1D-PMF was calculated using the existing umbrella windows (no additional umbrella sampling simulations were carried out). Also shown is the free-energy profile previously determined for WT Src kinase with its A-loop phosphorylated (blue curve) [13].

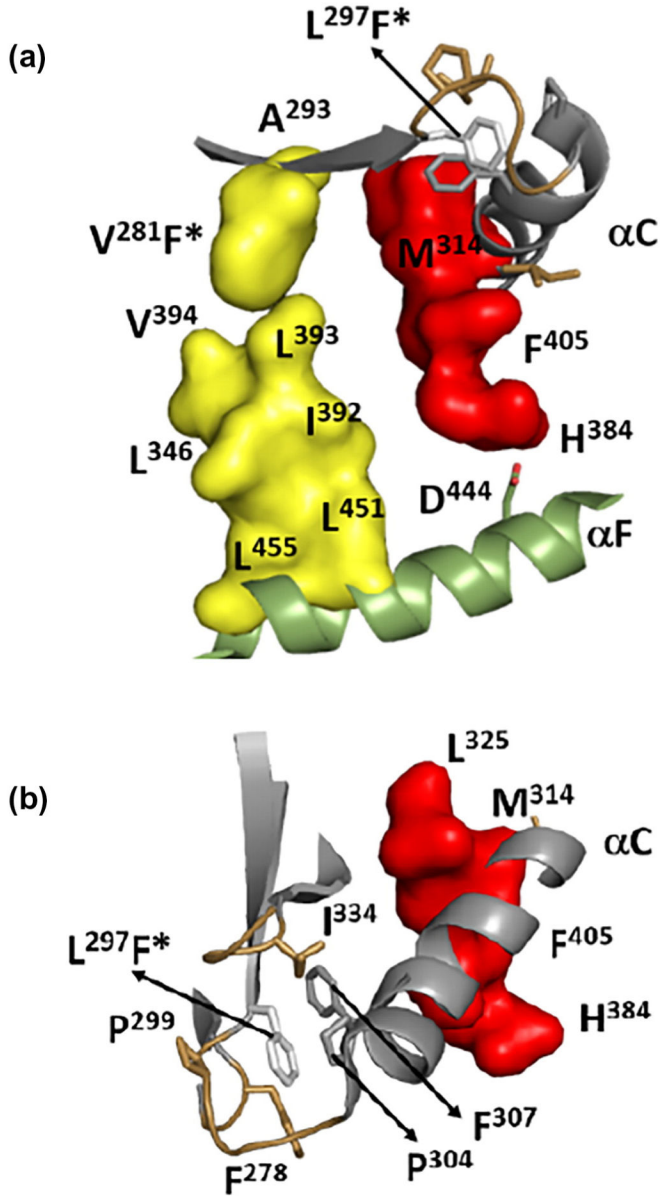

Fig. 4.

Structural details of the C- and R-spine in mutants of c-Src kinase. (a) Position of L297F in perspective of the two spines. (b) αC-helix serves as an integration hub of the hydrophobic unit and the R-spine.

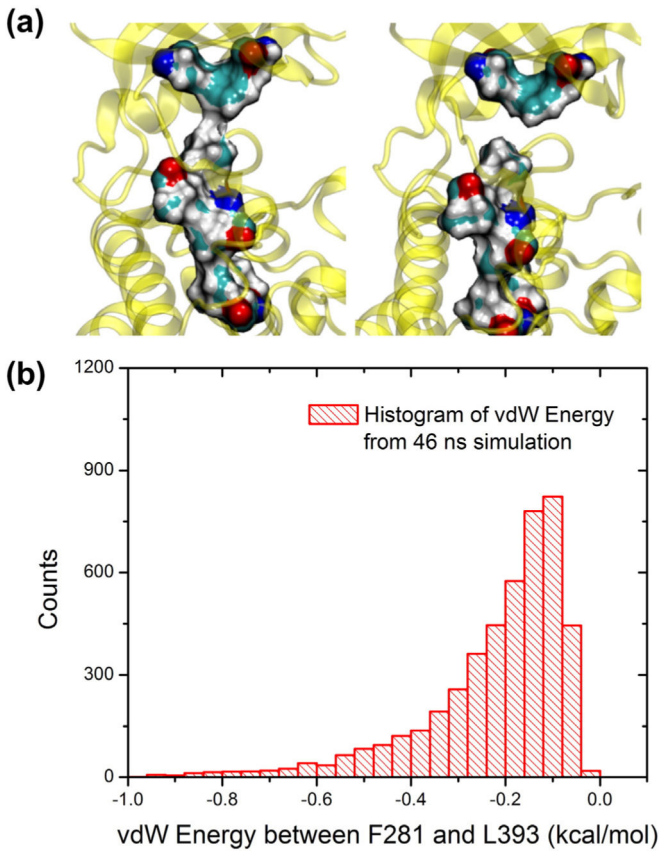

Fig. 5.

Analysis of the C-spine residues between the N-lobe and the C-lobe of the catalytic domain. (a) A view of the catalytic sites show that when F281 is connected with L393, the entire C-spine is completed (lower left), while a gap can be seen (lower right) if F281 and L393 are further away. (b) The histogram of the vdW energy between F281 and L393 is shown in the upper panel. On the one hand, the majority of the sample has non-zero energy, which means that F281 and L393 make contact throughout the equilibration stage. On the other hand, the median of the histogram is at ~−0.1 kcal/mol, suggesting that the contact is not very strong. A 1D-PMF as a function of F281–L393 vdW energy is carrying out.

Table 1.

Technical parameters of the 2D umbrella sampling calculations

	# windows	ns/ window	Total simulation time (μs)	k	d_w	W_{cutoff}
V281F–L297F	843	20	16.8	10	0.5	20
L297F (without ATP)	843	20	16.8	10	0.5	N/A
L297F (with ATP)	540	10	5.4	10	0.5	N/A
V281F	475	20	9.5	10	0.5	N/A
M314V	418	20	8.36	10	0.5	N/A
L297F–M314V	475	10	4.75	10	0.5	N/A

The total aggregated simulation time is 61.61 μs. The k stands for the force constant of the harmonic restraining potential and is in the unit of kcal/(mol · Å^2). The d_W stands for the spacing between two neighboring umbrella window in each dimension and is in the unit of Å. W_{cutoff} is the free-energy threshold in kcal/mol used by the self-learning adaptive algorithm [24].